BULLETIN OF THE POLISH ACADEMY OF SCIENCES
TECHNICAL SCIENCES, Vol. 71(1), 2023, Article number: e144578
DOI: 10.24425/bpasts.2023.144578

Experimental and numerical analyses of airflow around two cylinders angled to the direction of wind

Agnieszka PADEWSKA-JURCZAK*, Piotr SZCZEPANIAK, and Ryszard WALENTYŃSKI

Faculty of Civil Engineering, Department of Mechanics and Bridges, ul. Akademicka 5, 44-100 Gliwice, Poland

Abstract. The analyses aim to determine aerodynamic force coefficients in the case of airflow around two smooth or rough cylinders positioned at different angles to the direction of wind velocity. Such systems, for instance, may be part of a tubular water slide. The results were compared with the values of the interference coefficient of the cylinders arranged in a row included in Eurocode EN 1991 part 4. The aerodynamic forces of the cylinder systems were determined on the basis of experimental tests conducted in a wind tunnel. To verify the above results, CFD (computational fluid dynamics) simulations were prepared. An important observation is that for the angle of yaw $\beta = 0°$, the negative component of the lift force (lateral) f_y is shown, while for the other cases, the situation is opposite and the lateral force points outside the gap (upward). The second is that the results of aerodynamic drag for rough cylinders arranged in a row and calculated according to EN 1991 part 4 may be underestimated. The flow around the pair of smooth cylinders is quite different from that of the rough ones, because during the experiment the first falls into the critical flow regime, while the second has supercritical characteristics.

Key words: wind actions; CFD; FVM; ANSYS Fluent; wind tunnel test; water slides.

1. INTRODUCTION

Lightweight structural elements with circular cross sections and various nontypical shapes are applied in engineering on a large scale. One such example is water slides, frequently built of elements with a circular cross-section and the shape of a torus, a helix, a straight single pipe or several pipes arranged close to each other (see Fig. 1).

Fig. 1. General view of the water slides at Gino Paradise Bešeňová in Slovakia

Numerical and experimental analyses of the effect of wind on the arrangement of buildings or parallel cylinders are often found in the literature, for example, in [1–7]. The values of the κ factor, used to determine the increase in the aerodynamic force of cylinders arranged in a row, are proposed in Eurocode [1]. These problems were also discussed in some of the works of the [8, 9]. However, in the case of cylinders placed close to each other and with large Reynolds numbers Re, these values differ from those given in the literature. Furthermore, the results of the aerodynamic coefficients for a smooth cylinder differ from those for a cylinder with a rough surface. That kind of element is analysed rarely. The Eurocode also does not include the case of cylinders inclined to the wind direction. This paper also shows a problematic way of modelling flow with Re ranging from $1.33 \cdot 10^5$ to $2.62 \cdot 10^5$ around a system of two parallel cylinders.

The aerodynamic forces of the cylinder systems were determined on the basis of experimental tests carried out in a wind tunnel. To verify the above results, CFD (computational fluid dynamics) simulations were prepared.

A fragment of a rigid structure is analysed. The review of the results presented here is mainly limited to determining the aerodynamic forces of the cylinder systems, ignoring the possible vibration phenomena of a circular cylinder in the aerodynamic trace of another cylinder (interference galloping).

2. EXPERIMENTAL RESEARCH

Experimental research was carried out at the Faculty of Civil Engineering of the STU in Bratislava. The wind tunnel is designed with an open circuit scheme and constructed as a vacuum tunnel (Fig. 2). This means that the pressure in the out-of-operation tunnel is equal to the outside barometric pressure. During operation, the static pressure in the tunnel decreases, in contrast to the dynamic pressure.

*e-mail: agnieszka.padewska-jurczak@polsl.pl

Manuscript submitted 2022-06-29, revised 2022-12-13, initially accepted for publication 2023-01-11, published in February 2023.

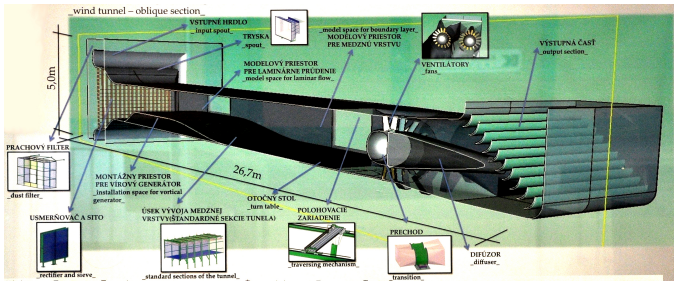

Fig. 2. Photo of the scheme of the wind tunnel at STU in Bratislava

The total width and height of the measurement space are $B = 2{,}600$ mm and $H = 1{,}600$ mm, respectively. The tunnel is divided into front (laminar flow) and rear (turbulent flow) test sections. The maximum available wind speed is approximately $w_{\mathrm{ref,max}} = 20$ m/s.

The subject of the investigation is the airflow around a system of two PVC pipes with diameter $\phi = 200$ mm and length $L = 2{,}400$ mm (Fig. 3). The gap between the top cylinder and the ceiling of the tunnel is constant and equals 350 mm, while the gap between the two pipes Δ varies. The set of cylinders is rotated horizontally by the yaw angle β equal to 0°, 15°, 30°, and 45° (see Fig. 4). Both smooth and rough cylinders were analysed, with the rough surface obtained by covering the pipes with a thick textured wallpaper (Fig. 5). According

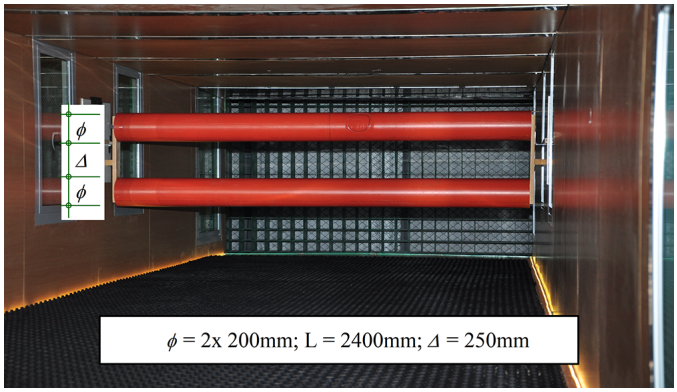

Fig. 3. Arrangement of the two cylinders in the wind tunnel

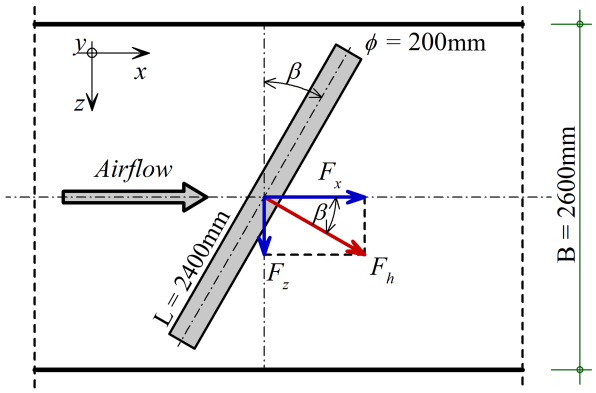

Fig. 4. Wind load on the yawed cylinders – the resultant drag force and its horizontal components (top view)

to the available wind speed, the Re value ranged from $1.33 \cdot 10^5$ to $2.62 \cdot 10^5$, calculated as for airflow around a single cylinder in open space.

Fig. 5. The detail of the rough cylinder

The front section of the tunnel is equipped with the reference sensor, the Prandtl sensor (Pitot static tube), to assess the dynamic air pressure and to measure the overall and static pressure. The distribution of wind pressure in the model was monitored using three DSA 3217 pressure scanners (Scanivalve) for 47 sample points (Fig. 6) (one sensor was out of order). Measurements are fully automated, that is, the temperature, barometric pressure, wind pressures, and the values of wind velocities values were automatically recorded and analysed in self-developed programs created in the LabView software.

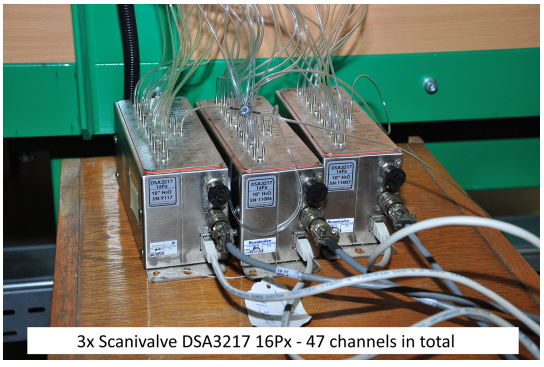

Fig. 6. Pressure scanners

Air temperature, density (ρ), and atmospheric pressure were, 17.6°C, 1.201 kg/m^3 and 100 680 Pa, respectively.

During the experiment, the pressure distribution $\Delta p(\alpha)$ was measured around a cross section located in the middle of the upper cylinder. The results of the calculation of the pressure coefficient c_p:

$$c_p = \frac{\Delta p(\alpha)}{q} = \Delta p(\alpha) \cdot \frac{2}{\rho w_{\mathrm{ref}}^2}, \tag{1}$$

obtained for the highest wind speed ($w_{\mathrm{ref}} \approx 19.2$ m/s, Re $\approx 2.6 \cdot 10^5$) are shown in Fig. 7. The important observation is that for

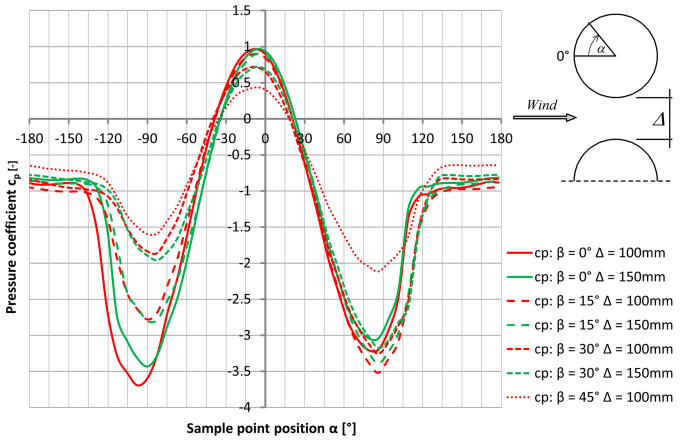

Fig. 7. Distribution of the pressure coefficient obtained for smooth cylinders and highest wind speed

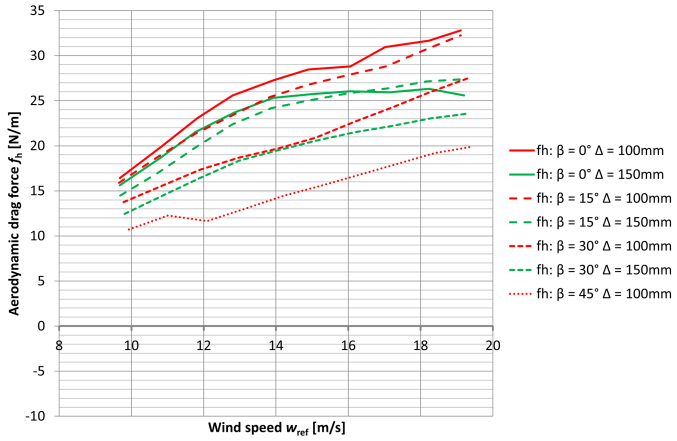

Fig. 8. Time-averaged horizontal component of aerodynamic drag force acting on the upper smooth cylinder for $\beta = 0° \div 45°$

the angle of yaw $\beta = 0°$ the highest suction values exist in the lower part of the top cylinder ($\alpha \approx -90°$, continuous lines), which generates a negative component of the lift (lateral) force f_y (pointing towards the gap between the cylinders)

$$f_y = \frac{F_y}{L} = -\int_{-\pi}^{\pi} \Delta p(\alpha) \frac{\phi}{2} \sin\alpha \, \mathrm{d}\alpha$$

$$\approx -\frac{\pi\phi}{47} \cdot \sum_{i=1}^{47} \Delta p(\alpha_i) \sin\alpha_i \,, \tag{2}$$

$$c_{fy} = \frac{f_y}{\phi \cdot q} = \frac{f_y}{\phi} \cdot \frac{2}{\rho \cdot w_{\mathrm{ref}}^2} \,. \tag{3}$$

While for the other cases the situation is opposite, and the lateral force points outside the gap (upward) (compare Fig. 10). The second observation is that the diagrams in Fig. 7 tend to flatten for the growing angle of the yaw, with a multiplication coefficient close to the value of $\cos^2(\beta)$.

Figures 8 and 9 present the horizontal component of the aerodynamic drag force f_h depending on the wind speed and the resulting force coefficients c_{fh} depending on the Reynolds number:

$$f_h = \frac{F_h}{L} = \int_{-\pi}^{\pi} \Delta p(\alpha) \frac{\phi}{2} \cos\alpha \, \mathrm{d}\alpha$$

$$\approx \frac{\pi\phi}{47} \cdot \sum_{i=1}^{47} \Delta p\,(\alpha_i) \cos\alpha_i \,, \tag{4}$$

$$c_{fh} = \frac{f_h}{\phi \cdot q} = \frac{f_h}{\phi} \cdot \frac{2}{\rho \cdot w_{\mathrm{ref}}^2} \,. \tag{5}$$

From an engineering point of view, Fig. 9 is more useful. In the paper [9] it can be found that in the cases of cylinders set perpendicular to the direction of wind velocity for the value of $\mathrm{Re} \geq 1.75 \cdot 10^5$ and $\Delta \geq 100$ mm, the graph shows values that are lower than those obtained from Eurocode [1] adequate for a single cylinder, where for the considered range of Reynolds

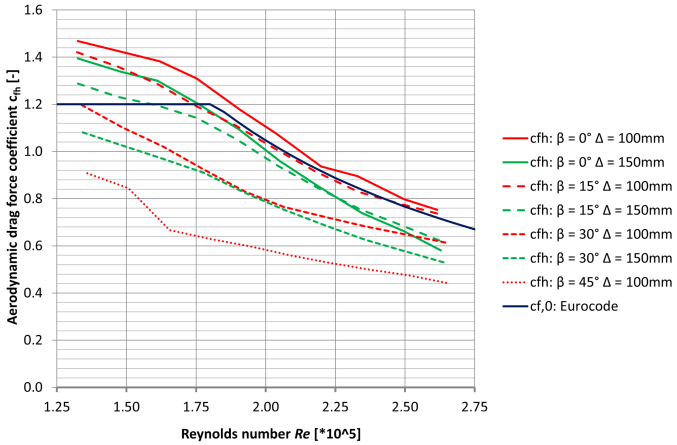

Fig. 9. Horizontal drag force coefficients for the upper smooth cylinder

numbers, the force coefficient is equal to:

$$c_{f,0} = \frac{0.11}{\left(\dfrac{\mathrm{Re}}{10^6}\right)^{1.4}} \leq 1.2. \tag{6}$$

Below these values, the force coefficient increases to 1.5. It is caused by the fact that bringing the cylinders together leaves less space between them, which creates a common aerodynamic path of flow and increases the difference of observed values of pressure between the windward and leeward surfaces of the cylinders. According to the classification of characteristic areas of aerodynamic interference of two cylinders presented by [10], cylinders located at a relative distance a/ϕ ($a = \Delta + \phi$) less than approximately 4.0, with a line passing through their centres perpendicular to the direction of flow, are subject to aerodynamic interference. Furthermore, in the area with $a/\phi < 2.0$, bistable flows occur, which means that the form of the airflow changes irregularly over time, causing vibrations. However, in the case of time-averaged measurements, it is hard to observe.

Figures 10 and 11 present the vertical component of the aerodynamic forces according to the speed of the wind and the time-averaged coefficients of the aerodynamic lateral force depending on the Re number. The highest values of vertical force are found for cylinders yawed horizontally from the direction of wind velocity by 30°, and are roughly 50% greater than the corresponding horizontal drag force. It can also be seen that for Re less than $2.25 \cdot 10^5$ values of the lateral force coefficient increase or are almost constant, while for higher values of the Re values they decrease (in the case of $\beta = 0^\circ$ very rapidly).

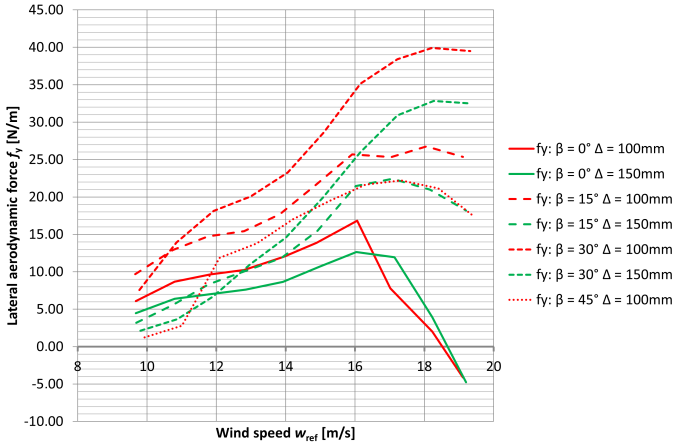

Fig. 10. Time-averaged vertical (lateral) component of aerodynamic force acting on the upper smooth cylinder for $\beta = 0^\circ \div 45^\circ$

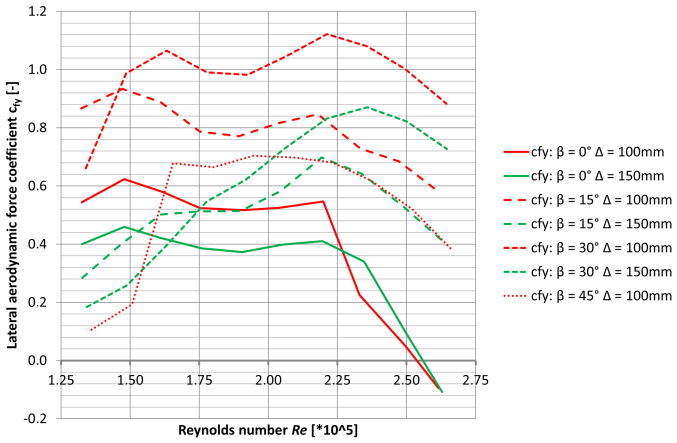

Fig. 11. Lateral force coefficients for the upper smooth cylinder

Contrary to previous observations, in the case of rough cylinders, it can be noticed that the results of the horizontal drag force coefficient (Figs. 12 and 13) do not change much with increasing Re number and depend mainly on the distance between the cylinders Δ and the yaw angle β. Similarly, the lateral force coefficient for rough cylinders is also almost independent of the Re number (in the range under consideration) and shows the highest values for cylinders positioned in a plane normal to the airflow direction (Figs. 14 and 15). Therefore, the flow around the pair of smooth cylinders is quite different from that of the rough ones, because during the experiment the first falls into the critical flow regime, while the second has supercritical characteristics.

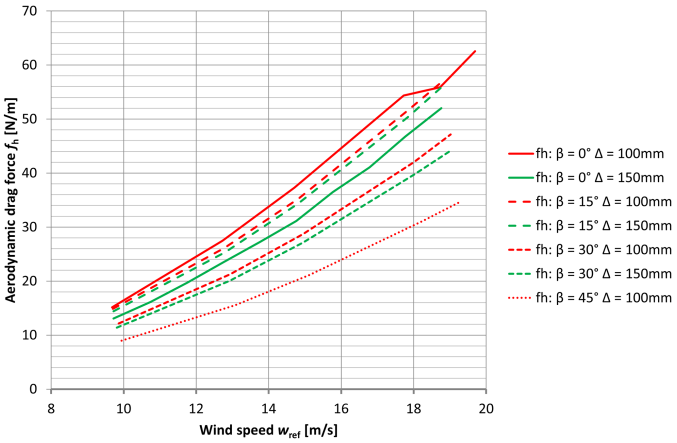

Fig. 12. Time-averaged horizontal component of aerodynamic drag force acting on the upper rough cylinder for $\beta = 0^\circ \div 45^\circ$

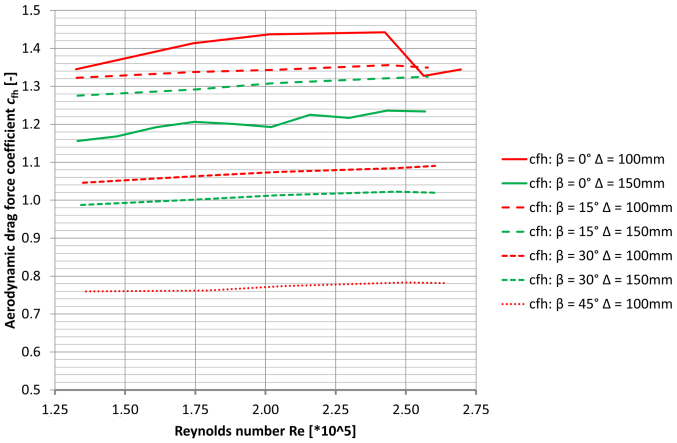

Fig. 13. Horizontal drag force coefficients for the upper rough cylinder

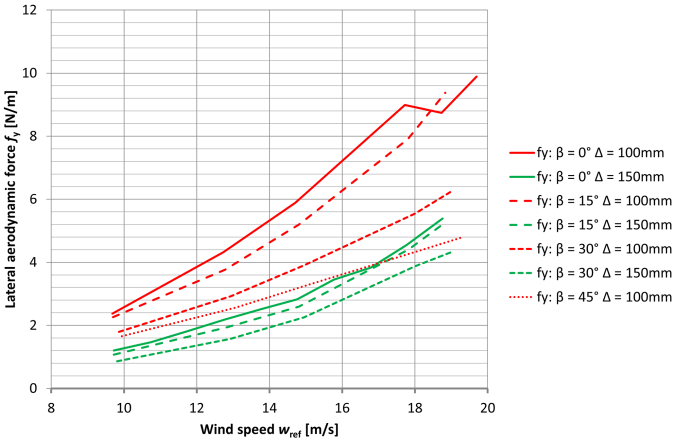

Fig. 14. Time-averaged vertical component of aerodynamic force acting on the upper rough cylinder for $\beta = 0^\circ \div 45^\circ$

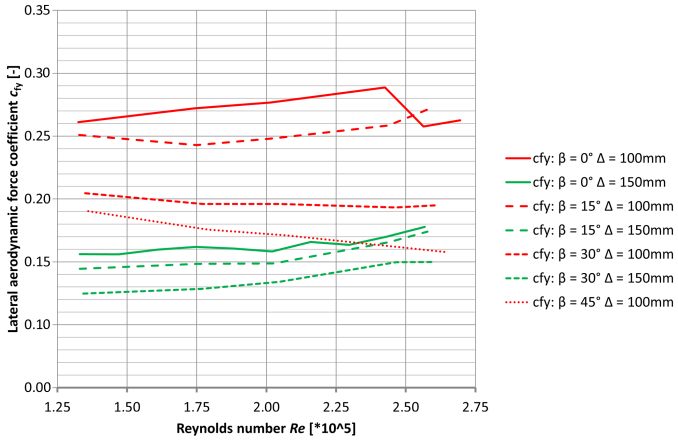

Fig. 15. Lateral force coefficients for the upper rough cylinder

3. NUMERICAL MODEL

The purpose of the numerical research is to simulate the experiment carried out in the wind tunnel and to compare the results.

To compare the results of the drag coefficient obtained in the wind tunnel and of the numerical analyses with the drag coefficients estimated according to [1], the following numerical analysis results refer to two cylinders placed perpendicular to the direction of the wind ($\beta = 0^\circ$). These are 2D analyses.

Figures 16 and 17 present the dimensions of the numerical model, taken from the wind tunnel, and the applied boundary conditions or the FVM mesh. Computational fluid dynamics (CFD) simulations were performed in the ANSYS Fluent program. The floor layer in the wind tunnel, made of a dimpled foil with a height of 20 mm, is considered. The coupled

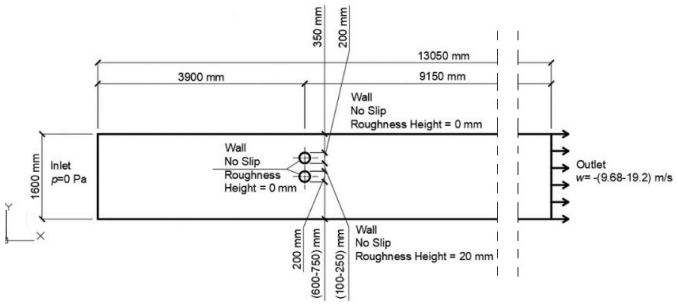

Fig. 16. Numerical model of airflow around two cylinders – dimensions and boundary conditions

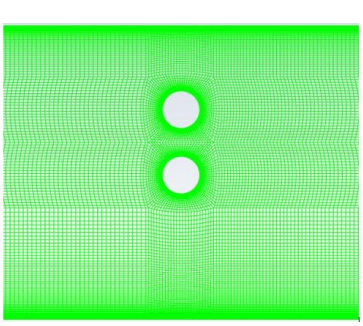

Fig. 17. Numerical model of airflow around two cylinders – FVM mesh

scheme, second order in spatial discretization and steady flow are used for the calculations. Various turbulence models were tested in [11]. The RANS Transition SST Turbulence Model is included. The modelling of airflow in the critical range of Re numbers around even a single cylinder is a complicated task.

The results of the aerodynamic drag force of the wind tunnel were used to calibrate the numerical models.

Although all types of flows fall within the critical range (see [12]), their nature is very different. Thus, it is necessary to adjust the parameters of the numerical model. This was also described in the paper [9]. Tables 1 and 2 show the parameters adopted when modelling the flow with different velocities around two cylinders with Δ of 150 mm and 200 mm. It contains, apart from the analysed wind speed and Reynolds number:

- Non-dimensional wall distance y^+ – checked values and finally accepted.
- The height of the element in the first layer of mesh near the walls of the cylinder h.
- $c_{f,1}/c_{f,2}/c_f$: obtained values of the drag coefficient for the upper cylinder, the lower cylinder, and the average value.
- Additional changed parameters.

Wind speeds are listed in reverse order because the model with the highest speed was used as the base. The modelling is mainly based on the selection of the height of the first FVM mesh elements. The quality of each mesh was checked in the Fluent program. The non-dimensional wall distance y^+ is adopted according to [13–17]. In the references mentioned possible ranges of values y^+ are included corresponding to each zone of the viscosity-affected region, among others. The paper [18] also reports on the development of a refined wall function strategy for the modelling of turbulent flow over rough surfaces. Models have significantly lower computational requirements (and coarse mesh) when using wall functions. The lower speed, the more parameters have to be changed. Following the adoption of all previous rules, the problem is converged. Residuals are decreased by three orders of magnitude. The net mass imbalance is less than 0.2% of the net flux through the domain. It means that when the present models are used, reliable results are obtained.

Figure 18 shows the pressure and velocity distributions around two cylinders set perpendicular to the wind speed determined from the numerical analysis. In the case of a speed of 19.2 m/s ($\mathrm{Re} = 2.6 \cdot 10^5$), a clear division is visible into the regions of the lower velocity and pressure values (in front of the cylinders) and the region of higher values (between the cylinders). In the case of the lowest speed, this division is hardly perceptible and is difficult to model. A pair of vortexes in the wake of the two cylinders was observed, similar to the flow behind a cylinder. A similar flow is included in the work [19].

Quote [1]: "For vertical circular cylinders in a row arrangement, the force coefficient $c_{f,0}$ depends on the direction of the wind related to the row axis and the relationship of distance a and diameter b as defined in Table 7.14. The force coefficient, c_f, for each cylinder may be obtained by expression (7.22):

$$c_f = c_{f,0} \cdot \psi_\lambda \cdot \kappa, \tag{7}$$

Table 1
Parameters assumed when modelling the flow around the cylinders with Δ of 150 mm

w [m/s] / Re number [–]	y^+ checked [–] / y^+ finally adopted [–]	h [m]	$c_{f,1}/c_{f,2}/c_f$ [–]	Additional information
$19.2/2.6\cdot10^5$	20, 34, 50, 82, 100, 120, 150 / 100	$3.2\cdot10^{-3}$	0.62 / 0.59 / 0.6	The flow Courant number was changed from 1 to 1000. However, this did not significantly affect the drag coefficient results. Switching to curvature correction in the viscous model did not change the results.
$18.23/2.5\cdot10^5$	from 30 to 100 / 80	$3.2\cdot10^{-3}$	0.68 / 0.64 / 0.66	
$17.4/2.3\cdot10^5$	from 30 to 80 / 60	$2.2\cdot10^{-3}$	0.71	
$16.4/2.0\cdot10^5$	from 20 to 50 / 40	$15\cdot10^{-4}$	0.86	
$14.98/1.9\cdot10^5$	20, 30 / 30	$12\cdot10^{-4}$	1.0	
$13.92/1.9\cdot10^5$	from 5 to 40 / 15	$6.6\cdot10^{-4}$	1.1	The area of viscosity influence is in the blending region.
$12.85/1.7\cdot10^5$	from 10 to 20 / 10	$4.6\cdot10^{-4}$	1.21 / 1.21 / 1.21	The flow turned out to be more complicated due to the inability to fully use the wall functions. Three models were tested: Laminar, Transition SST, and Reynolds stress. The Transition SST model was chosen. The flow Courant number was changed from 0.1 to 200. FCN and explicit relaxation factors were equal to 1.
$11.77/1.6\cdot10^5$	from 1 to 10 / 10	$5.0\cdot10^{-4}$	1.33	The explicit relaxation factors equal to 1 were left, as there was a calculation error for other values. The change in FCN in the range of 0.1 to 5 also did not bring the expected improvement in the c_f values. Curvature correction was enabled in the Transition SST model.
$10.8/1.5\cdot10^5$	from 1 to 10 / 8	$4.2\cdot10^{-4}$	1.36	
$9.68/1.3\cdot10^5$	from 1 to 10 / 8	$4.8\cdot10^{-4}$	1.39	

Table 2
Parameters assumed when modelling the flow around the cylinders with Δ of 200 mm

w [m/s] / Re number [–]	y^+ checked [–] / y^+ finally adopted [–]	h [m]	$c_{f,1}/c_{f,2}/c_f$ [–]	Additional information
$19.2/2.6\cdot10^5$	100	$3.2\cdot10^{-3}$	0.5 / 0.48 / 0.49	Explicit relaxation factors (momentum and pressure) had to be increased from 0.75 to 1.
$18.23/2.5\cdot10^5$	80	$3.2\cdot10^{-3}$	0.53	The value of explicit relaxation factors had to be changed.
$17.4/2.3\cdot10^5$	from 40 to 80 / 50	$18\cdot10^{-4}$	0.68	

where: $c_{f,0}$ is the force coefficient of cylinders without free end flow (single cylinder), ψ_λ is the end-effect factor (equal to 1 for "infinite cylinders"), κ is the factor that increases aerodynamic drag given in Table 7.14 (for the most unfavourable wind direction)." This direction is not specified in [1]. Article [20] shows that higher coefficient values of the coefficient κ were obtained with this arrangement of two cylinders when the axis connecting their centres was perpendicular to the direction of the wind speed (cylinders positioned next to each other) than in the case of the axis (one cylinder behind the other) or in intermediate settings. Experimental analyses of the drag coefficient of the system of two cylinders positioned at different angles to the wind speed direction, performed by the Authors, confirmed these observations.

The κ coefficient depends on the relative distance between the cylinders. For the cases analysed in this paper, the κ coefficient is 1.15. The $c_{f,0}$ coefficient can be estimated according to Fig. 7.28 in [1]. This coefficient depends on the Re number and the equivalent roughness of the surface of the cylinder k/b. During the experiment, the smallest relative distance between the cylinders a/ϕ is equal to 1.5, where $a = \Delta + \phi$.

Tables 3 and 4 show the κ results obtained from numerical or experimental analyses and estimated based on the standard [1]. The drag coefficient of a single cylinder is assumed to be equal to value given in [1].

Tables 3 and 4 show the κ results obtained from experimental analyses and estimated based on the standard [1] for smooth cylinders. The drag coefficient of a single cylinder is assumed

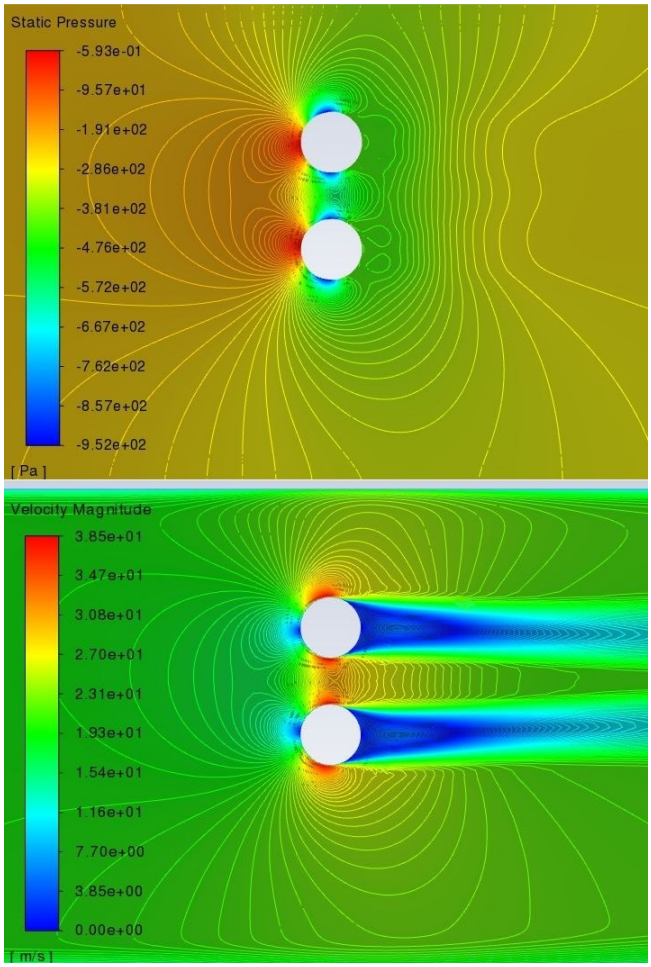

Fig. 18. Distribution of pressure and velocity around two cylinders set perpendicular to the wind at $w_{\text{ref}} = 19.2$ m/s and $\Delta = 150$ mm

to be equal to the value given in [1] for a smooth cylinder.Only in the case of the lowest of the wind velocities and $\Delta = 150$ mm, the difference in κ results is imperceptible. In other cases, the κ-factor is slightly overestimated. If it comes to $\Delta = 100$ mm and Re $= 1.3 \cdot 10^5$ the interference coefficient κ is 1.22 and is greater than those given in [1]. For yawed cylinders, these values are lower.

Table 3

Comparison of the κ results obtained from experimental analyses and estimated on the basis of standard [1] in the case of smooth cylinders for $\Delta = 100$ mm

Re number	κ from experimental analyses	κ on the basis of the standard [1]
$1.3 \cdot 10^5$	$1.47/1.2 = 1.22$	1.15
$1.7 \cdot 10^5$	$1.31/1.2 = 1.09$	1.15
$1.9 \cdot 10^5$	$1.19/1.12 = 1.06$	1.15
$2.0 \cdot 10^5$	$1.08/1.05 = 1.03$	1.15
$2.3 \cdot 10^5$	$0.91/0.83 = 1.10$	1.15
$2.5 \cdot 10^5$	$0.81/0.77 = 1.05$	1.15
$2.6 \cdot 10^5$	$0.75/0.72 = 1.04$	1.15

Table 4

Comparison of the κ results obtained from numerical or experimental analyses and estimated on the basis of standard [1] in the case of smooth cylinders for $\Delta = 150$ mm

Re number	κ from experimental analyses	κ on the basis of the standard [1]
$1.3 \cdot 10^5$	$1.39/1.2 = 1.16$	1.15
$1.7 \cdot 10^5$	$1.20/1.2 = 1.0$	1.15
$1.9 \cdot 10^5$	$1.10/1.12 = 0.98$	1.15
$2.0 \cdot 10^5$	$0.86/1.05 = 0.82$	1.15
$2.3 \cdot 10^5$	$0.71/0.83 = 0.82$	1.15
$2.5 \cdot 10^5$	$0.66/0.77 = 0.86$	1.15
$2.6 \cdot 10^5$	$0.60/0.72 = 0.83$	1.15

It should be noted that the British annex to the EN 1991-1-4 standard lacks guidelines to determine the value of the interference factor for a/ϕ lower than 2.5. According to research by other Authors, this limit could even be changed to $a/\phi < 3.0$. Furthermore, quoting the Eurocode: "For cylinders near a plane surface with a distance ratio $zg/b < 1.5$ (distance between the ground and the wall of the cylinder over the diameter of the cylinder) special advice is necessary." This is analogous to cylinders placed close to each other. For angled cylinders, these values are similar to those given in [1].

Tables 5 and 6 show the κ results obtained from experimental analyses and estimated based on the standard [1] for rough cylinders. The drag coefficient of a single cylinder is assumed to be equal to the value given in [1] for $k = 1$ mm (the height of the wallpaper bump). It should be noted that in the cases of the lower Re numbers, the drag coefficient for a single rough cylinder is equal to the results for a smooth cylinder, according to [1]. Furthermore, the κ factor itself, according to [1], does not depend on the roughness of the surface. In the case of rough cylinders, the differences in the κ coefficient between the values obtained in the wind tunnel and the Eurocode [1] are remarkably high. For the number Re equal to $2.7 \cdot 10^5$ and

Table 5

Comparison of the κ results obtained from the experimental analyses and estimated according to the standard [1] in the case of rough cylinders for $\Delta = 100$ mm

Re number	κ from experimental analyses	κ on the basis of the standard [1]
$1.3 \cdot 10^5$	$1.34/1.2 = 1.12$	1.15
$1.7 \cdot 10^5$	$1.41/1.2 = 1.18$	1.15
$2.0 \cdot 10^5$	$1.44/1.05 = 1.37$	1.15
$2.5 \cdot 10^5$	$1.33/0.89 = 1.48$	1.15
$2.7 \cdot 10^5$	$1.34/0.9 = 1.49$	1.15

Table 6
Comparison of the κ results obtained from the experimental analyses and estimated on the basis of standard [1] in the case of rough cylinders for $\Delta = 150$ mm

Re number	κ from experimental analyses	κ on the basis of the standard [1]
$1.3 \cdot 10^5$	$1.16/1.2 = 0.97$	1.15
$1.7 \cdot 10^5$	$1.21/1.2 = 1.00$	1.15
$2.0 \cdot 10^5$	$1.19/1.05 = 1.13$	1.15
$2.5 \cdot 10^5$	$1.23/0.89 = 1.38$	1.15

$\Delta = 100$ mm, the relative difference is even 30%. The values of κ for the rough cylinders obtained according to [1] can be underestimated. On the other hand, it should be checked whether the values of the drag coefficient for a single cylinder, with the appropriate Re numbers and surface roughness, are not overestimated in Eurocode.

4. CONCLUSIONS

The purpose of the analyses was to determine aerodynamic force coefficients in the case of airflow with high velocity near structures with circular cross-sections, arranged in rows, e.g., elements of water slides. The results were compared with the information on the design of such elements or structures contained in the Eurocode [1].

First, the aerodynamic forces of the cylinder systems were determined on the basis of experimental tests carried out in a wind tunnel. To verify the results, CFD (computational fluid dynamics) simulations were prepared.

Several important new findings have been observed. For the angle of yaw $\beta = 0^\circ$ the highest suction values exist in the lower part of the top cylinder ($\alpha \approx -90^\circ$), which generates a negative component of the lift (lateral) force f_y. While for the other cases the lateral force points outside the gap (upward). The highest vertical forces occur in the case of cylinders yawed horizontally from the direction of wind velocity by 30°, and are roughly 50% higher than the corresponding horizontal drag force. It is also shown that the values of κ for rough cylinders obtained according to [1] can be underestimated. On the other hand, it should be checked whether the values of the drag coefficient for a single cylinder, with the appropriate Re numbers and surface roughness, are not overestimated in Eurocode. The flow around the pair of smooth cylinders is quite different from that of the rough ones, because during the experiment the first falls into the critical flow regime, while the second has supercritical characteristics.

The other observation is that the distribution of the pressure coefficient obtained for smooth cylinders and the highest wind speed tends to flatten for the growth angle of yaw, with a multiplication coefficient close to the value of $\cos^2(\beta)$. It can also be seen that for Re less than $2.25 \cdot 10^5$ values of the lateral force coefficient increase or are almost constant, while for higher values of the Re values they decrease (in the case of $\beta = 0^\circ$ very rapidly).

In the case of rough cylinders, it can be observed that the results of the aerodynamic force coefficients do not change much with increasing Re number and depend mainly on the distance between the cylinders Δ and the angle β.

Modelling the flow with Re from $1.33 \cdot 10^5$ to $2.62 \cdot 10^5$ around an obstruction is a difficult task. The numerical model was created on the basis of research in the wind tunnel. Although all types of flows fall within the critical range, their nature is very different. Therefore, different parameters of the model had to be adopted. For a speed of 19.2 m/s (Re $= 2.6 \cdot 10^5$), a clear division is visible into regions with lower velocity and pressure values (in front of the cylinders) and a region with higher values (between the cylinders). In the case of the lowest speed, this division is hardly perceptible and is difficult to model.

The results of the interference coefficient of the cylinders arranged in a row, increasing their aerodynamic resistance, were compared with the values given in [1]. When designing a structure according to the Eurocode, many inaccuracies and limitations can be found. The drag coefficient of a single cylinder is assumed to be equal to the value given in [1]. Only in the case of the lowest of the analysed wind velocities and $\Delta = 150$ mm for the smooth cylinder, the difference in κ results is imperceptible. In other cases, the κ-factor is slightly overestimated in [1]. If it comes to $\Delta = 100$ mm and Re $= 1.3 \cdot 10^5$ the interference coefficient κ is 1.22 and is greater than those given in [1]. For yawed cylinders, these values are lower.

However, the blockage ratio, equal to up to 25%, is also of immense importance because it could have a significant impact on the airflow velocity distribution and, therefore, the pressure results. However, the Authors wanted to obtain as highest Re number as possible, because the final goal is to model a structure similar to the one presented in Fig. 1, where the Re exceeds $2 \cdot 10^6$. The drag coefficient values are actually lower after the blockage ratio is reduced to 5%. However, the numerical model has exactly the same dimensions as the wind tunnel. In the cases analysed in the wind tunnel and described in this paper, the values of the aerodynamic interference coefficients in the case of a smooth cylinder are similar to those given in the standard [1]. Furthermore, changing the calculation to a transient flow causes a new increase in the value of the drag coefficient.

To make a more complete analysis, it would be necessary to determine the aerodynamic interference coefficients of various cylinder systems and different diameters. In addition, it may be necessary to consider, for example, connectors or platforms with which water slides are equipped in the calculations. The phenomenon of vibrations of a circular cylinder, in the trace of another cylinder (the so-called interference galloping), should also be investigated.

REFERENCES

[1] CEN, *EN 1991-1-4 Eurocode 1: Actions on structures – Part 1-4: General actions – Wind actions with National Annex*. Brussels, Warszawa: CEN, PKN, 2005.

[2] W. Jester and Y. Kallinderis, "Numerical study of incompressible flow about fixed cylinder pairs," *J. Fluids Struct.*, vol. 17, pp. 561–577, 2003, doi: 10.12989/was.2020.30.1.015.

[3] C. W. Park and S.J. Lee, "Flow structure around two finite circular cylinders located in an atmospheric boundary layer: side-by-side arrangement," *J. Fluids Struct.*, vol. 17, pp. 1043–1058, 2003, doi: 10.12989/was.2020.30.1.015.

[4] E. Błazik-Borowa and J. Szulej, "Interferencja aerodynamiczna walców w ustawieniu bocznym do kierunku wiatru," *Fizyka Budowli w Teorii i Praktyce*, vol. 1, pp. 31–38, 2005.

[5] D. Yeo and N. Jones, "Computational Study on 3-D Aerodynamic Characteristics of Flow around a Yawed, Inclined, Circular Cylinder," NNSEL Report Series Report No. NSEL-027, Urbana-Champaign, 2011.

[6] K. Gumowski, O. Olszewski, M. Poćwierz, and K. Zielonko-Jung, "Comparative analysis of numerical and experimental studies of the airflow around the sample of urban development," *Bull. Pol. Acad. Sci. Tech. Sci.*, vol. 63, no. 3, pp. 729–737, 2015, doi: doi: 10.1515/bpasts-2015-0084.

[7] V.L. Nguyen and D.K. Ho, "Numerical investigation of vortex wake patterns of laminar flow around two side-by-side cylinders," *Arch. Mech. Eng.*, vol. 69, no. 3, pp. 541–565, 2022, doi: 10.24425/ame.2022.141517.

[8] A. Padewska, P. Szczepaniak, and A. Wawrzynek, "Porównanie sił aerodynamicznych działających na połowę torusa i dwa walce o tej samej długości," *Modelowanie Inżynierskie*, vol. 29, no. 60, pp. 52–57, 2016.

[9] A. Padewska-Jurczak, P. Szczepaniak, and R. Walentyński, "Experimental and numerical analyses of airflow around two cylinders angled to the direction of wind," in *Lightweight Structures in Civil Engineering Contemporary Problems. Monograph from Scientific Seminar*, 2022.

[10] M. Zdravkovich, "Review of interference-induced oscillations in flow past two parallel circular cylinders in various arrangements," *J. Wind Eng. Ind. Aerodyn.*, vol. 28, pp. 183–199, 1988, doi: 10.1016/0167-6105(88)90115-8.

[11] A. Padewska, "Pogłębiona analiza numeryczna oddziaływania wiatru na obiekty budowlane o nietypowym kształcie i układzie," Silesian University of Technology, 2016.

[12] M. Coutanceau and J.-R. Defaye, "Circular Cylinder Wake Configurations: A Flow Visualization Survey," *Appl. Mech. Rev.*, vol. 44, no. 6, pp. 255–305, 1991, doi: 10.1115/1.3119504.

[13] J. Anderson, *Computational Fluid Dynamics. The basics with applications*. USA: McGraw-Hill, Inc., 1995.

[14] ANSYS Inc., "ANSYS Documentation for Release 15/Customer Training Material." ANSYS Inc., USA, 2013.

[15] T. Jiyuan, H. Guan, and L. Chaoqun, *Computational Fluid Dynamics. A Practical Approach*. USA: Elsevier Inc., 2008.

[16] H. Versteeg and W. Malalasekera, *An Introduction to computational fluid dynamics: the finite volume method*. Pearson Education Ltd., 2007.

[17] D. Wilcox, *Turbulence modelling for CFD*. USA: DCW Industries, 2006.

[18] K. Suga, T.J. Craft, and H. Iacovides, "Extending an Analytical Wall-Function for Turbulent Flows Over Rough Walls," *Eng. Turbul. Model. Exp.*, vol. 6, pp. 157–166, 2005.

[19] D. Li, Q. Yang, X. Ma, and G. Dai, "Free Surface Characteristics of Flow around Two Side-by-Side Circular Cylinders," *J. Mar. Sci. Eng.*, vol. 6, no. 3, p. 75, 2018, doi: 10.3390/jmse6030075.

[20] J.A. Żurański, "Wpływ interferencji aerodynamicznej na obciążenie wiatrem stalowych kominów wieloprzewodowych – Aerodynamic interference effects on wind loads of multi-flue steel chimneys," *Prace Instytutu Techniki Budowlanej*, vol. 2–3, pp. 37–64, 2000.